Efficient Bottom-Up Image Segmentation Using Region Competition and the Mumford-Shah Model for Color and Textured Images

Yongsheng Pan J. Douglas Birdwell Seddik M. Djouadi
Department of Electrical and Computer Engineering
University of Tennessee, Knoxville
ypan@lit.net birdwell@lit.net djouadi@ece.utk.edu

Abstract

Curve evolution implementations [3][23] [25] of the Mumford-Shah functional [16] are of broad interest in image segmentation. These implementations, however, have initialization problems [6] [25]. A mathematical analysis of the initialization problem for the Chan-Vese implementation [3] [25] is provided in this paper. The initialization problem is a result of the non-convexity of the Mumford-Shah functional and the top-down hierarchy of the model's use of global region information in the image. Based on the analysis, efficient implementation methods are proposed for the Chan-Vese models [3] [25]. The proposed methods do not have to solve PDEs and thus work fast. The advantages of level set methods, such as automatic handling of topological changes, are preserved. These methods work well for images without strong noise. Initialization problems, however, still exist. A bottom-up image segmentation method is proposed that alleviates the initialization problem, based on region competition and the Mumford Shah functional [16]. This algorithm extends the method in [15], and is able to automatically and efficiently segment objects in complicated images. Using a bottom-up hierarchy, the method avoids the initialization problem in the Chan-Vese model and works for images with multiple junctions and color images. It is then extended to textured images using Gabor filters and fractal methods. Experimental results show that the proposed method works well and is robust to the effects of noise.

1 Introduction

Curve evolution methods [1] [2] [3] [5] [6] [7] [8] [10] [11] [13] [14] [19] [20] [23] [25] [26] [27] are widely used in image segmentation problems. These methods drive one or more initial curve(s), based on image gradient and/or region information , to the boundaries of objects in an image. These methods are derived using variational methods, and are implemented using finite difference approximations to PDEs and level sets [9] [17].

In curve evolution methods, region-based geometric methods [3] [6] [8] [13] [19] [23] [25] [26] have several advantages. They can deal with topological changes automatically, outperforming parametric methods such as [10] and [27]. Utilization of global region information stabilizes their responses to local variations (such as weak edges and noise) in comparison to gradient-based geometric methods [1] [2] [11] [14] [20].

Region-based geometric methods, however, have some limitations. First, most have initialization problems [6] [25]: different initial curves produce different segmentations. Second, these methods have difficulty with complicated images with multiple junctions. Top-down hierarchical methods [13] [18] [23] or multiple coupled evolving curves [25] [26] have been used to segment multiple objects. Top-down hierarchical methods are time-consuming. In the worst case, n curve evolutions must be performed to segment an image with n objects. Coupled evolving curves usually introduce high computational loads, and techniques must be used to ensure that no pixels are left over or segmented twice.

A mathematical analysis of the initialization problem for the Chan-Vese models [3] [25] is provided in this paper. From that analysis, the initialization problem is shown to originate from both the non-convexity of the Mumford-Shah functional and the top-down hierarchical way that region information is utilized. Based on the way of the Chan-Vese models to utilize region information, efficient implementation methods for the Chan-Vese models are proposed. The methods do not have to solve PDEs. The computational load of curve evolution is thus greatly reduced. The proposed method bears some similarities to [20], but the proposed method is region-based rather than gradient-based as in [20]. It is more straightforward to build region information to drive curve evolution. More complicated issues, such as sensitivity to noise which is not considered in [20], are discussed. The proposed methods, although still have initialization problems, work efficiently for images without strong noise. They can also deal with complicated images such as triple junctions. Initialization problems, however, remain.

From the mathematical analysis, provided in section 2, a bottom-up hierarchical algorithm may therefore be helpful. Region growing methods shown in [15] is a good example. Every pixel in the image is treated as a region at the beginning in [15]. Regions are merged if the merging decreases the well-posed case of the Mumford-Shah functional [16]. It avoids the initialization problem and works very fast. However, this method is sensitive to local variations such as weak edges. The region competition method proposed in [27] utilizes region competition to combine snakes, region growing and MDL(Minimum Description Length)/Bayes methods. Although this has been shown to work for color and textured images, the proper manual selection of seed points for region growing at the first stage is required, limiting its applicability. Tek and Kimia [21] proposed another bottom-up segmentation method using reaction-diffusion bubbles. These bubbles are hypothesized as fourth order shocks and are randomly initialized in homogeneous areas of the image. These bubbles grow, shrink, split and disappear to capture objects in the image. The method, however, has difficulty with multiple junctions.

In this paper, an efficient bottom-up image segmentation method is proposed that uses region competition and the Mumford-Shah functional. The method reserves the advantages of the method in [15]: it avoids the initialization problem of the Chan-Vese models; it works for complicated images and is efficient; it is robust to the effects of noise; its efficiency can be enhanced using multi-scale methods and parallelization. The proposed method outperforms [15] in the case of local variations.

The paper is organized as follows. In section 2, the Mumford-Shah functional and the Chan-Vese models are introduced. The initialization problem of the Chan-Vese models is analyzed in section 3. Based on the analysis, a fast curve evolution method that does not require solution of a PDE is proposed in section 4. A novel image segmentation method based on region growing and the Mumford-Shah functional is proposed in section 5. In section 6, implementation issues are discussed. An analysis of experimental results is provided in section 7. Section 8 provides summary with conclusions and future work.

2 Background

The Mumford-Shah functional [16] is introduced first in this section, followed by the analysis of the bi-modal and multiphase Chan-Vese models

2.1 The Mumford-Shah Model

Let I_0 be a function representing the image to be segmented and I be a differentiable function representing the segmented image. Both I_0 and I are defined on a planar domain R. Let R_i be disjoint connected open subsets of R with piecewise smooth boundaries and let Γ be the union of the portions of the boundaries of R_i inside R. Then the Mumford-Shah functional is defined as

$$E(I,\Gamma) = \mu^2 \iint_R (I - I_0)^2 dxdy + \iint_{R-\Gamma} \|\nabla I\| dxdy + \nu|\Gamma| \tag{1}$$

where $|\Gamma|$ represents the total length of Γ, and μ and ν are positive constant. The first term in (1) asks I approximates I_0; the second term asks that I doesn't vary much in each region; the third term asks the boundaries are as short as possible. All three terms work together to make the functional meaningful.

The functional in (1) is not necessarily well-posed. In most cases, a special case of (1), in which I is restricted to be piecewise constant, is applied. The special case of the Mumford-Shah functional, which is well-posed, takes the following form

$$E(\Gamma) = \Sigma_i \iint_{R_i} (I_0 - mean_{R_i}(I_0))^2 dxdy + \nu|\Gamma| \tag{2}$$

Although the functional in (2) is well-posed and may have a global minimum, it is not convex and may have numerous local minima. This is the underlying reason that the Chan-Vese models, which will be introduced next, have the initialization problem.

2.2 The Bi-modal Chan-Vese Model

The Chan-Vese model [3] [25] is the curve evolution implementation of a special case of the Mumford-Shah model [16]. The bi-modal Chan-Vese model [3] minimizes the following energy functional:

$$\begin{aligned} F(c_1, c_2, C) = {} & \mu \cdot Length(C) \\ & + \lambda_1 \iint_{inside(C)} |I(x,y) - c_1|^2 dxdy \\ & + \lambda_2 \iint_{outside(C)} |I(x,y) - c_2|^2 dxdy \end{aligned} \tag{3}$$

where I is the original image, C is the evolving curve, and c_1 and c_2 are selected as the average values of pixels inside and outside C, respectively. μ, λ_1 and λ_2 are positive constants. Both λ_1 and λ_2 are usually taken as 1. These two parameters, therefore, are neglected in the following derivations.

The energy functional (3) is minimized by solving the following PDE:

$$\psi_t = \delta_\epsilon(\psi)[\mu \cdot \kappa - (I - c_1)^2 + (I - c_2)^2] \tag{4}$$

where ψ is the level set representation of the evolving curve C, which means $C = \{(x, y)|\psi(x, y) = 0\}$. κ represents the curvature of the evolving curve. $\delta_\epsilon(\psi) = \epsilon/(\pi(\epsilon^2+\psi^2))$ and ϵ is a positive constant.

From (4), the evolution of the curve is influenced by two terms. The curvature term κ regularizes the curve and makes it smooth during evolution. The region term $-(I-c_1)^2 + (I-c_2)^2$ affects the motion of the curve. The initialization of the curve affects curve evolution through this term.

2.3 The Multiphase Chan-Vese Model

The bi-modal Chan-Vese model is applicable only for bi-modal images. The multiphase Chan-Vese model [25] has been proposed for more complex images. In this model, two or more coupled curves evolve simultaneously to segment images with multiple objects. Consider a four-phase Chan-Vese model, in which two coupled curves ψ_1 and ψ_2 evolve according to coupled Euler-Lagrange equations.

Suppose the initial curves divide the image into four regions: $R_{00} = \{\psi_1 < 0, \psi_2 < 0\}$, $R_{10} = \{\psi_1 > 0, \psi_2 < 0\}$, $R_{01} = \{\psi_1 < 0, \psi_2 > 0\}$, $R_{11} = \{\psi_1 > 0, \psi_2 > 0\}$, as shown in Fig. 4 (a). Let c_{00}, c_{10}, c_{01}, and c_{11} be the average intensities inside R_{00}, R_{10}, R_{01}, R_{11}, respectively. The evolution of ψ_1 and ψ_2 follows the Euler-Lagrange equations:

$$\begin{aligned}\frac{\partial \psi_1}{\partial t} &= \delta_\epsilon(\psi_1)\{\nu\kappa_1 - ((I_0 - c_{11})^2 - (I_0 - c_{01})^2)H(\psi_2) \\ &- ((I_0 - c_{10})^2 - (I_0 - c_{00})^2)(1 - H(\psi_2))\}\end{aligned} \tag{5}$$

$$\begin{aligned}\frac{\partial \psi_2}{\partial t} &= \delta_\epsilon(\psi_2)\{\nu\kappa_2 - ((I_0 - c_{11})^2 - (I_0 - c_{10})^2)H(\psi_1) \\ &- ((I_0 - c_{01})^2 - (I_0 - c_{00})^2)(1 - H(\psi_1))\}\end{aligned} \tag{6}$$

where $\kappa_1 = \nabla \cdot (\frac{\nabla\psi_1}{|\nabla\psi_1|})$ and $\kappa_2 = \nabla \cdot (\frac{\nabla\psi_2}{|\nabla\psi_2|})$ are the curvatures of the evolving curve ψ_1 and ψ_2. $H(\cdot)$ is the Heaviside function: $H(x) = 1$ when $x > 0$ and $H(x) = 0$ when $x < 0$.

It can be seen from (5) that the evolution of ψ_1 determines a boundary comprised of two parts: the part between R_{00} and R_{10} where $\psi_2 < 0$, and the part between R_{01} and R_{11} where $\psi_2 > 0$. The first part evolves due to region information in R_{00} and R_{10}. The evolution of the second part is driven by region information between R_{01} and R_{11}. Similar observations can be made for ψ_2. In this manner, the multiphase Chan-Vese model divides the image into several smaller regions and performs curve evolution based on region information in these regions.

3 The Initialization Problem of The Chan-Vese Model

An analysis is provided in this section for the initialization problem of the Chan-Vese models. Based on the background information in section 2, three observations can be made about the initialization problem.

First, initialization determines which local minimum of the energy functional (2) is achieved. Initialization in the Chan-Vese models provides the starting point for the minimization of the energy functional. Since the energy functional may have multiple local minima, and the Euler-Lagrange method is a gradient-descent method, a local minimum may be reached, for example, if the initial value is chosen to be closer to one of the local minima than the global minimum. Fig. 3 illustrates this fact. The initialization in Fig. 3(a) causes the global minimum of (2) to be found where all the objects are segmented. The initialization in Fig. 3(c), however, is closer to a local minimum of (2) than to the global minimum, and one object is not segmented as a result in Fig. 3(d). The solutions to the Chan-Vese model may go through different intermediate states for different initializations even if they achieve the same local minimum. An illustration is provided in Fig. 1 and Fig. 2.

Second, the way the Chan-Vese model utilizes region information helps to formulate the initialization problem. In the Chan-Vese models, information from different regions are competing to evolve the curve. If initialization causes the total influence of multiple regions on the curve to be zero, nothing is segmented. Although the multiphase Chan-Vese model introduces computation between multiple small regions, initialization is still a problem without prior information about the image.

Third, coupling between evolving curves may magnify the effects of initialization and introduce more computational load. Fig. 4 illustrates this fact. For the initialization in (a), curve evolution based on only region information can not reach a local minimum, as shown in (d). It can be seen from (e)-(h), however, that every part of the evolving curve converges to a local minimum. Although the curvature term may finally drive the curves to a local minimum, the coupling introduces extra computation and makes the segmentation time-consuming. Therefore, it is useful to decouple the evolving curves in the multiphase Chan-Vese model for better segmentation results [6].

A more detailed mathematical analysis is shown in the following to illustrate the above statements. Consider a piecewise constant bi-modal image. Suppose there are n_1 pixels in the background of the image, among which

$m_1 (0 \leq m_1 \leq n_1)$ pixels lie inside the initial curve. Suppose there are n_2 pixels in the foreground of the image, among which $m_2 (0 \leq m_2 \leq n_2)$ lie inside the initial curve. All the pixels in the background (foreground) take $u_1 (u_2)$ as their intensity values. Obviously, $m_1 + m_2 > 0$ for all initializations.

The the average intensity inside the evolving curve is

$$c_1 = (m_1 u_1 + m_2 u_2)/(m_1 + m_2), \tag{7}$$

and the average intensity outside the evolving curve is

$$c_2 = ((n_1 - m_1) u_1 + (n_2 - m_2) u_2)/((n_1 - m_1) + (n_2 - m_2)). \tag{8}$$

The region terms $-(I - c_1)^2 + (I - c_2)^2$ for points on the evolving curve in the foreground and the background are

$$(u_2 - c_2)^2 - (u_2 - c_1)^2 = K_0 K_2 (m_2 n_1 - m_1 n_2)(u_1 - u_2)^2 \tag{9}$$

$$(u_1 - c_2)^2 - (u_1 - c_1)^2 = -K_0 K_1 (m_2 n_1 - m_1 n_2)(u_1 - u_2)^2, \tag{10}$$

where $K_0 = 1/\{(n_1 - m_1 + n_2 - m_2)(m_1 + m_2)\}$, $K_1 = (n_2 - m_2)/(n_1 - m_1 + n_2 - m_2) + m_2/(m_1 + m_2)$ and $K_2 = (n_1 - m_1)/(n_1 - m_1 + n_2 - m_2) + m_1/(m_1 + m_2)$, respectively. K_0, K_1 and K_2 are positive for any initialization.

From (9) and (10), it can be seen that the region term for points on the foreground part of the evolving curve is opposite in sign to that on the background part of the evolving curve. Therefore, if one part of the evolving curve expands, the remaining part will have to shrink and vice versa. Without loss of generality, set $\psi > 0$ inside the evolving curve and $\psi < 0$ outside the evolving curve. Then three cases may occur, depending upon different initializations. If $m_2 n_1 - m_1 n_2 > 0$ $(m_2/n_2 > m_1/n_1)$, then the foreground part of the curve expands, and the background part shrinks. The curve evolves into the foreground and segments the object from the foreground, as shown in Fig. 1. If $m_2 n_1 - m_1 n_2 < 0$ $(m_2/n_2 < m_1/n_1)$, then the foreground part of the curve shrinks and the background part expands. The curve evolves into the background and segment the object from the background, as shown in Fig. 2,. Finally, if $m_2 n_1 - m_1 n_2 \approx 0$, then the influence of the region term on the curve evolution is small at first. The curve is expected to evolve very slowly and may segment nothing.

It can be seen from the above analysis that initialization affects curve evolution in the Chan-Vese model. The results from Fig. 1 and Fig. 2 illustrate this point. Although in Fig. 1 and Fig. 2, the same segmentation results are achieved, in complicated cases, different initializations may generate different segmentation results, as shown in Fig. 3. Both initializations (a)(c) in Fig. 3 satisfy $m_2/n_2 > m_1/n_1$, making the foreground part of the evolving curve expand and the background part shrink. Since the upper object is not included in the initialization in (c), it is not segmented using that initialization. This suggests that every object in the image should have at least one pixel included in the initial curve for good segmentation. For the Chan-Vese model, good choices for the initialization would be the boundaries or multiple bubbles. Multi-modal images can exacerbate the initialization problem. This holds even for the multiphase Chan-Vese model [25], as shown in [6]. In the worst case, the Chan-Vese model can fail to segment any object if the total influence of the region information on the initial curve is zero, as is shown in Fig. 8 (b1) and (b2).

The Chan-Vese model uses a top-down hierarchical method for segmentation, and global region information is utilized only on the evolving curve in the model. The initialization problem is a consequence of this. A bottom-up hierarchical method, which makes use of local information, may reduce the initialization problem and allow its application to more complex images. A new image segmentation method, which is based on region growing and the Mumford-Shah model, is proposed in section 5. Before the introduction of the new method, however, we propose a very fast curve evolution method for the Chan-Vese model, based on the analysis in this section.

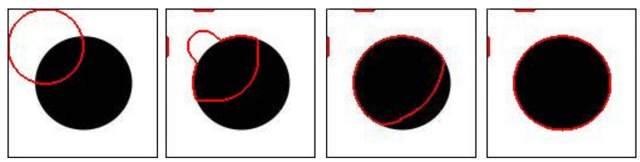

(a) (b) (c) (d)

Figure 1. Example of the initialization problem, where $m_2/n_2 = 0.21$ is larger than $m_1/n_1 = 0.16$. (a)(b)(c)(d) show the curve evolution after 0, 10, 60 and 234 iterations separately.

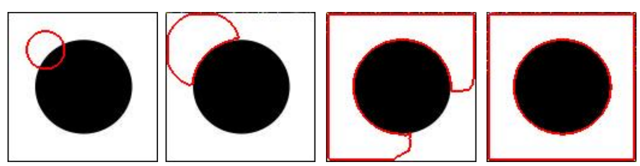

(a) (b) (c) (d)

Figure 2. Example of the initialization problem, where $m_2/n_2 = 0.036$ is smaller than $m_1/n_1 = 0.065$. (a)(b)(c)(d) show the curve evolution after 0, 10, 600 and 1182 iterations separately.

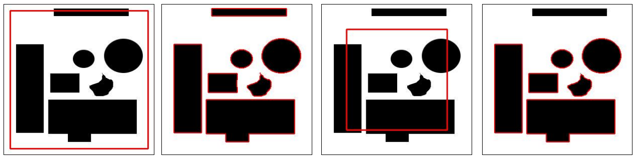

Figure 3. Different initialization in the Chan-Vese model may generate different segmentation results. (a) and (c) represent images with different initializations. (b) and (d) are the segmentation results corresponding to (a) and (c) respectively. The top rectangle is not segmented in (d).

4 Fast Curve Evolution Methods Without Solving PDEs

The Chan-Vese models are usually implemented by solving PDEs, such as the level set equations [9] [17] and Poisson equations [25]. These methods are computationally intense, although they are theoretically sound. Fast implementation methods are proposed for both the bi-modal and the multiphase Chan-Vese models in this section. A mathematical analysis of the region information in the bimodal Chan-Vese model is provided first, which provides the concept for a fast implementation evolution method for that model that does not require solving PDEs. The proposed method is extended to the decoupled multiphase Chan-Vese model, as provided in [6].

4.1 Fast Implementation of the Bi-modal Chan-Vese Model

From the equations (9) and (10), the following observations can be acquired for the bi-modal Chan-Vese model: First, the region term $-(I-c_1)^2+(I-c_2)^2$ of the foreground has the opposite sign to the region term of the background for any initialization. Second, for any point strictly inside the foreground or the background, its region term will has the same sign as the terms for its neighboring points. Third, only the boundary points will have neighboring points with region terms different in sign.

The observations shown above hold for all bi-modal images without strong noise. This information can be used to construct an efficient evolution of the initial curve. A list of points, instead of a narrow band of points in classical methods [9] [17], is utilized to represent the evolving curve. Without loss of generality, suppose the points inside the initial curve are set to have positive ψ value. For any point in the list, if this point and all its neighboring points have positive region terms, then at that point the curve will expand according to (4). We only need to remove this point from the list, and add to the list those neighboring points that have negative ψ values. Correspondingly, if a point on the list and all its neighboring points have negative terms, then the curve will shrink at that point. We need to remove this point from the list and add to the list those neighboring points that have positive ψ values. Otherwise, the boundary has been reached, and nothing needs to be done.

Up to this point, the regularization term in (4) has not been used in the proposed method. As proved in [12], curve evolution based on curvature $\partial C/\partial t=\kappa N$ is equivalent to a nonlinear analogy to Gaussian smoothing. Thus Gaussian smoothing can be applied after each iteration of curve evolution to smooth the curve.

4.2 Fast Implementation of the Multiphase Chan-Vese Model

It seems straightforward to extend the proposed method to the multiphase Chan-Vese model. In this case, two or more curves are initialized and then evolved according to the region information. Gaussian smoothing is utilized to regularize the evolving curves. However, the coupling between the evolving curves in the multiphase Chan-Vese model, as can be seen from (5) and (6), may cause the evolving curves stop at a local minimum [6] [25]. An illustration is provided below.

In Fig. 4, (b) shows an image with initialized curves. Let ψ_1 be the red curve and ψ_2 be the green curve. Both curves are initialized positive inside and negative outside. (c) shows the segmentation result using the coupled multiphase Chan-Vese model. The blue lines in (c) means the red curve and the green curve both stop there. It can be seen that parts of the evolving curves do not stop at object boundaries, and only a local minimum is reached. (d) shows the final location of the green part of the evolving curve, which corresponds to the part of ψ_2 in the region $\psi_1>0$. This part of the curve, which evolves under the direction of region information in the area of $\psi_1>0$, reaches its local minimum. Similar results can be achieved for the other three parts of the evolving curves. The final result, however, is not a real local minimum of the Mumford-Shah functional (2). In other words, multiphase curve evolution in this case reaches a “false” local minimum here. This problem arises from the coupling of the evolving curves.

Decoupled models [6] have been proposed to solve the problem. In this model, only one curve is evolved at a time. The first curve ψ_1 separates the original image into two regions $\{\psi_1>0\}$ and $\{\psi_1<0\}$. The second curve ψ_2 evolves based on the results of the first curve, and may segment the original image into three or four regions, such as $\{\psi_1>0,\psi_2<0\}$. This procedure is repeated until all the objects in the original image are segmented. The evolving curves in decoupled models are more likely to stop at object boundaries because they do not evolve simultaneously.

Decoupled models in [6] reduce the effects of coupling, but they solve PDEs for image segmentation, which is computationally intense. The fast implementation method proposed in the above section can be extended for decoupled multiphase models. Consider the four-phase case of the Chan-Vese model. Two curves C_1 and C_2 are initialized, and evolve in consecutive iterations. In each iteration, the implementation method for the bi-modal case is utilized. For the first iteration, the curve C_1 evolves using region information $R_1 = ((I_0 - c_{11})^2 - (I_0 - c_{01})^2)H(\psi_2) - ((I_0 - c_{10})^2 - (I_0 - c_{00})^2)(1 - H(\psi_2))$ as in Eqn. (5). After the first iteration is completed, the other curve C_2 evolves using region information $R_2 = -((I_0 - c_{11})^2 - (I_0 - c_{10})^2)H(\psi_1) - ((I_0 - c_{01})^2 - (I_0 - c_{00})^2)(1 - H(\psi_1))$ as in Eqn. (6). Gaussian smoothing is utilized for regularization.

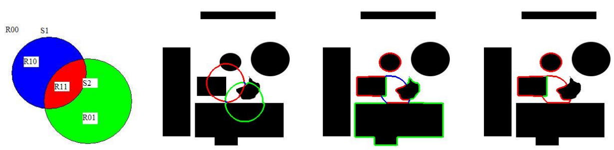

(a) (b) (c) (d)

Figure 4. Coupling between curve evolution may enlarge initialization problems. (a) Multiphase Chan-Vese model. (b) Initialization. (c) Segmentation results. (d) show the positions of one part of the evolving curves in (c).

5 Image Segmentation Using Region Competition and the Mumford-Shah Functional

In this section, an image segmentation method is proposed based on region region competition and the Mumford-Shah model. First, an explanation of the Chan-Vese models [3] [25] is provided based on the concept of region competition. The proposed segmentation method is then described. Finally, an extension to color and textured images is developed.

5.1 Region Competition in the Chan-Vese Models

The Chan-Vese models [3] [25] minimize an energy functional by evolving an initialized curve. Curve evolution can be interpreted as the result of competition between the foreground and the background. This idea is similar to the method proposed in [27]. Curve evolution stops when the competition is in equilibrium.

Consider, for example, the bi-modal case in section 3, and let $\psi > 0$ inside the evolving curve. The curve evolves according to the competition between the foreground region and the background region. When the evolving curve reaches the boundary of the object, $m_1 = 0$, $m_2 = n_2$, $c_1 = u_2$, and $c_2 = u_1$. The region terms calculated using the boundary points in the foreground are $(u_2 - c_2)^2 - (u_2 - c_1)^2 = (u_2 - u_1)^2 > 0$, and the region terms for the boundary points in the background are $(u_1 - c_2)^2 - (u_1 - c_1)^2 = -(u_2 - u_1)^2 < 0$. These region terms are equal in magnitude and opposite in sign. The competition is balanced, and the evolving curve stops at the boundary of the object.

5.2 Image Segmentation Based on Region Competition and the Mumford-Shah Functional

The proposed image segmentation method is designed to minimize the well-posed case of the Mumford-Shah functional [16] using bottom-up region growing and region competition. The energy functional takes the form:

$$E(\Gamma) = \sum_i \iint_{R_i} (I - c_i)^2 dxdy + \nu \cdot \Gamma \qquad (11)$$

where Γ represents the length of object boundaries, I represents the image to be segmented, c_i represents the average intensity of the ith region R_i and ν is a constant parameter.

As mentioned in [16], the energy functional (11) tends to segment images into piecewise constant regions, which gives an opportunity for minimization using region growing. The proposed method works as follows: Every pixel in the image is initially its own region. A region is merged with a neighboring region if this action will decrease the energy functional (11). In this way, the neighboring regions of any selected current region are competing with each other to reduce the energy functional. After two regions are merged, the intensity of each pixel in the merged region is set to the average intensity of the regions. The process is repeated until no region merging occurs and no further reduction of the value of the energy functional is possible. A mathematical description of region merging is given below.

Consider two neighboring regions Ω_1 and Ω_2 in the image. Suppose Ω_1 and Ω_2 contain n_1 and n_2 pixels respectively, with c_1 and c_2 as their average intensities. These two regions have Γ pixels in common as their boundaries. If the regions are merged, the average intensity would be $c = (n_1c_1 + n_2c_2)/(n_1 + n_2)$. The energy functionals before and after region merging can be evaluated:

$$E_{prev} = \iint_{\Omega_1} (I - c_1)^2 dxdy + \iint_{\Omega_2} (I - c_2)^2 dxdy + \nu \cdot \Gamma \qquad (12)$$

$$E_{after} = \iint_{\Omega_1} (I-c)^2 dxdy + \iint_{\Omega_2} (I-c)^2 dxdy \quad (13)$$

. The energy difference, therefore, is

$$E_{after} - E_{prev} = 2V_1(c_1 - c) + 2V_2(c_2 - c) + n_1(c^2 - c_1^2) \quad (14)$$
$$+ n_2(c^2 - c_2^2) - \nu \cdot \Gamma$$

where $V_1 = \iint_{\Omega_1} Idxdy$ and $V_2 = \iint_{\Omega_2} Idxdy$. Region merging is performed only if the energy difference is smaller than zero, reducing the value of the energy functional.

The ideas so far are very similar to the method in [15]. Two extension are made to improve their performances. On the one hand, during region growing, irregular boundaries may be generated, especially in images with strong noise. Regularization of region boundaries is, therefore, necessary. Gaussian smoothing is utilized, and is performed only when the region becomes larger than a specified threshold.

On the other hand, region growing is not enough for energy minimization in some cases. Although the merges of two regions may increase the energy functional, moving their common boundaries may decrease the energy functional. Thus, region competition on the boundaries between neighboring regions can be beneficial. In fact, region growing can be taken as a special case of the region competition. This idea is similar to the ideas [21] [27] and the Chan-Vese models presented in [3] [25]. But there are differences. First, region competition in the present case results in changes between regions, not the evolution of curves. Second, region competition is performed only when region growing can not decrease the energy functional, lowering the computational burden.

Several methods may be applied for region competition, such as in [3] and [27]. The bimodal Chan-Vese model [3] is a good choice because the geometric curve evolution in [3] can handle topological changes automatically. But [3] may be time-consuming. In the implementation, therefore, the fast curve evolution methods proposed in section 4 are applied. Since they do not solve PDEs, they are very efficient.

In the proposed method, region information is used in a manner that is similar to the Chan-Vese models [3] [25], but initialization problem can be avoided and complicated cases such as multiple regions and triple junctions are automatically handled, because of the bottom-up hierarchical approach of the proposed method. The proposed method can be seen as an extension of the multiphase Chan-Vese model when numerous initial curves are introduced so that every pixel in the image is taken as a region. It can also be viewed as a method to select the starting point for energy minimization to try to reach the the global minimum.

5.3 Existence of the Solution of the Proposed Method

In the proposed method, the image is discretely sampled as pixels, and the energy functional is approximated by a finite sum. Then there are a finite number of possible combinations for image segmentation. This holds not only for the region growing method in [15], but also for the proposed region competition method. The characteristics of region growing are kept in the proposed method, although post-processing is added. Minimum of the approximated energy functional, therefore, exists. As proved in [15], the minimum can be achieved by region growing, and thus by the proposed region competition method.

5.4 Extension to Color Images and Textured Images

The proposed method can be extended in a straightforward manner to color or textured images. Several color models, such as the one used in [27], can be chosen for the extension. The RGB color model is utilized here for simplicity. For textured images, Gabor filters [22] [24] or fractal methods [4] are utilized here to preprocess the textured images. The proposed methods are then applied to segment the processed images using the following energy functional

$$E(\Gamma) = \sum_{j=1}^{n} \sum_{i} \iint_{R_i} (I_j - c_{ij})^2 dxdy + \nu \cdot \Gamma \quad (15)$$

where n represents the number of features ($n = 3$ for color images) and j represents the indices of the features.

The implementation of the proposed method for color and textured images is similar to that for intensity images. The only difference lies in the calculation of the region information.

6 Implementation Issues

The key issue for the implementation of the proposed method is how to select an appropriate value for ν for a specified image. Intuitively, ν should be large enough to suppress noise and small enough not to merge regions separated by edges with high gradients. We show that the value of ν should also be related to the size of competing regions.

Consider two extreme cases for the region growing problem of section 5.2. First, if $V_1 = n_1 c_1$, $V_2 = n_2 c_2$ and $n_1 = n_2 = n$, then $c = (c_1 + c_2)/2$, and

$$E_{after} - E_{prev} = 1.5 \cdot n(c_1 - c_2)^2 - \nu \cdot \Gamma \quad (16)$$

If, on the other hand, $V_1 = n_1 c_1$, $V_2 = n_2 c_2$ and $n_1 >> n_2$, then $c \approx c_1$, and

$$E_{after} - E_{prev} \approx n_2(c_1 - c_2)^2 - \nu \cdot \Gamma \quad (17)$$

In both cases, the energy change as regions grow is highly related to the size of competing regions (n in (16) or n_2 in (17)). It is very difficult to select the proper value of ν if many regions of different sizes are competing at the same time.

Since the proposed method assigns a region to each pixel at the beginning, the above problem can be solved by restricting the maximum size of a region after each iteration. For example, the largest region after the first traverse of the whole image is set to 2 pixels. The image is then segmented into numerous regions containing two pixels after the first traverse. The largest region after the second traverse of the image is then set to 4 pixels. Now almost all competing regions contain 2 pixels and the image will be segmented into regions of 4 pixels, and so on. In this way, most competing regions have the same size, and the selection of the value of ν may be less affected by the sizes of the regions.

Suppose the variance of noise in an intensity image is σ^2, and the gradient of the region boundaries is expected to be g_0 ($g_0 > \sigma$); then the value of ν can be selected such that $\sigma^2 < \nu < g_0^2$. For color images, the value of ν can be selected such that $3\sigma^2 < \nu < 3g_0^2$. It is usually acceptable to choose $\nu = 1000$ for intensity images and $\nu = 3000$ for color images.

7 Experimental Results

Experimental results from the proposed method are shown in this section. The proposed method is implemented on a computer which has two Intel(R) Pentium(R) 3.2GHz CPUs, 2G bytes RAM, and runs the Red Hat Enterprise Linux operating system. The CPU times given in this paper are the sums of system CPU times and user CPU times. The system CPU time is usually very small, typically 0.01 - 0.08 seconds.

7.1 Experimental Results of the Fast Implementation Methods

The proposed fast implementation method is efficient compared to the classical method solving PDEs [9] [17], as can be seen from Fig. 5, which shows that the proposed method is much faster and achieves the same segmentation results for both synthetic and real images. Fig. 5 (a1)-(a3) demonstrate that the proposed method is able to automatically handle topological changes.

Fig. 6 shows segmentation results using the proposed method for complicated images. (a)-(d) shows the segmentation of triple junctions using the proposed method for the decoupled multiphase Chan-Vese model. The red initial curve in (a) is evolved first, and the result is shown in (b). The green curve shown in (b) is evolved in the second iteration, and the result is shown in (c). (d) shows the final segmentation result. The results show that the proposed method works well for images with multiple junctions. However, only a local minimum is reached in this case, which means the initialization problem still exists in the fast implementation method.

The effects of noise on the proposed fast implementation method are illustrated in Fig. 7. Fig. 7 (a)-(c) show the segmentation of an image with medium noise. Although the noise affects the process of curve evolution, as can be seen in Fig. 7 (b), the object in the image is successfully segmented in Fig. 7 (c). In this case region information has to be updated after every iteration to reduce the effects of noise, which is not required in the image of Fig. 5. Fig. 7 (d) shows the curve evolution result after 100 iterations for an image with strong noise. The proposed method fails in this case. The reason is that the noise in the image is so strong that it changes the sign of the region term R. The curve can not evolve in the proper direction from the sign of the region term.

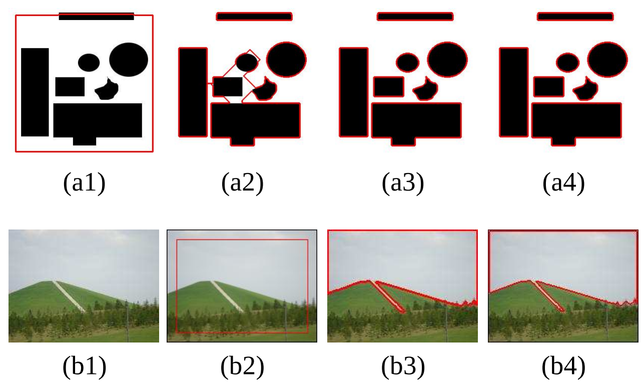

Figure 5. Comparison of the proposed fast implementation method to the classical method solving PDEs [9] [17]. (a1) An image (300 * 300) with initial curve. (b1) Intermediate result using the proposed method. (c1) Segmentation result of the proposed method, CPU = 0.51s. (d1) Segmentation result of the Chan-Vese model by solving PDEs, CPU = 11.98s. The new method provides a 23 times speed-up. (b1) An original image (200 * 150). (b2) Initial curve of (b1). (b3) Segmentation result of the proposed method, CPU = 0.34s. (b4) Segmentation result of the Chan-Vese model, CPU = 30.835s. The new method provides almost 100 times speed-up.

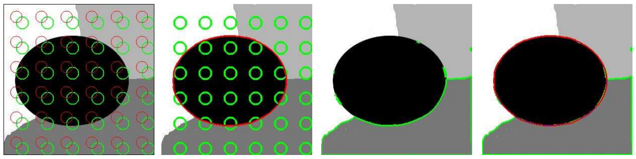

(a) (b) (c) (d)

Figure 6. Fast decoupled curve evolution for complicated images. (a) Original image (300 * 300) with initializations. (b) Segmentation results after the first iteration. (c) Segmentation result after the second iteration. (d) Final segmentation result, CPU = 1.960s.

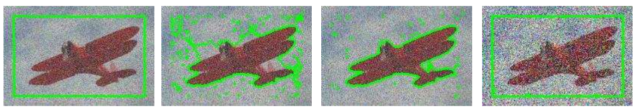

(a) (b) (c) (d)

Figure 7. Effects of noise on the proposed fast implementation method. (a) An image with medium noise. (b) Curve evolution after 44 iterations. (c) Segmentation results of (a), CPU = 0.3s. (d) Curve evolution after 100 iterations for an image with strong noise. The proposed method fails in (d).

7.2 Experimental Results of the Bottom-Up Segmentation Methods

Experimental results of the proposed bottom-up segmentation methods are provided in this subsection. Fig. 8 represents the comparison of the proposed method and the Chan-Vese model. (a1) shows the image to be segmented. The image contains one background region (intensity 128) and 4 foreground regions (intensity 32, 64, 192, 224 counterclockwise) of equal size. The segmentation result in (a2) shows that the proposed is very efficient (1.9s). The Chan-Vese model fails for the initialization shown in (b1). Since the effects of the region information on the curve are zero, the curve evolves very slowly, driven by the curvature. After more than 13 seconds, the initial curve evolves into (b2) and will shrink to a point in the end.

Fig.9 shows the comparison between the region competition method and the region growing method in [15]. For images with weak edges (a)(d), segmentation results of the improved method (b2)(c2)(e2) are much better than the results of the previous method. The boundaries between regions are more regularized and the results are closer to the original image. It can also be seen that both methods are very efficient.

Fig. 10 demonstrates the ability of the proposed region competition method to deal with images with multiple junctions. The initialization problem can occur happen for the Chan-Vese model, as shown in [6]. The proposed method generates very good segmentation results with high efficiency.

Fig. 11 shows the stability of the proposed method with respect to noise. It can be seen that the proposed method works very well for images with strong noise. The results also shows that a larger ν is required, and the segmentation process becomes longer for images with stronger noise.

In Fig. 12, the extension of the proposed method to color images is tested. Images in Fig. 12 (a1)(a2) are designed to have the same intensity so that they can not be segmented just using intensity. By means of the color information, the proposed method successfully segments objects with different colors.

Fig. 13 shows the effects of ν on the segmentation results. The image has four regions. The pixels are randomly chosen and independent, with Gaussian distribution $N(60, 40^2)$, $N(110, 40^2)$, $N(160, 40^2)$, and $N(210, 40^2)$. By the discussion in section 6, the choice of ν should satisfy $40^2 < \nu < 50^2$. The results in Fig. 13 show that the proposed method works for a wider range of ν. From the results in Fig. 13 (b)(c)(d), it can be seen that the segmentation time becomes shorter with increasing ν, while at the same time the object boundaries become coarser. This can be explained by the fact that regions are more likely to be merged with larger ν values. In practice, a compromise has to be made between efficiency and accuracy.

Experimental results for complicated real images are provided in Fig. 14. Gaussian smoothing is not utilized here since these images are of good quality. It can be seen that the proposed method is very efficient, even for complex images. Post-processing may be necessary for better results.

In Fig. 15, Gabor filters are utilized for texture description. (a3)(b3) show the outputs of Gabor filter (a2)(b2) applied to original textured images (a1)(b1). The proposed segmentation method is then applied on (a3)(b3), which generates final segmentation results (a4)(b4). Experimental results in (a4)(b4) show that regions of textures are segmented very well. Multiple Gabor filters may also be applied on (a1)(b1). The selection of parameters for Gabor filters and the combination of their outputs for a textured image are topics under investigation.

8 Conclusions and Future Work

In this paper, a mathematical analysis of the initialization problem of the Chan-Vese model is provided. This analysis shows that the initialization problem is caused by the top-down manner in which region information is used. A new bottom-up image segmentation method is proposed to solve this problem. It is based on region growing, region competition, and the Mumford-Shah functional. This method works well for complex images. It is very efficient, easy to implement and robust to noise. Experimental results show this method is able to quickly segment complex images. A fast curve evolution method is also proposed for the Chan-Vese model. This method does not need to solve PDEs and works very well for images without strong noise.

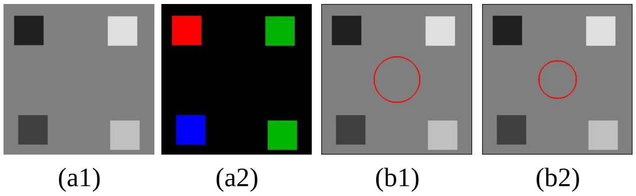

Figure 8. Comparison of the proposed region competition method and the Chan-Vese model for images with multiple regions. (a1) A gray image (256 by 256) with average intensity 128. (a2) Segmentation of the proposed method, ν=1000, CPU =1.9s. (b1) A gray image with the initialized curve. (b2) Segmentation using the Chan-Vese model, CPU = 13.03s.

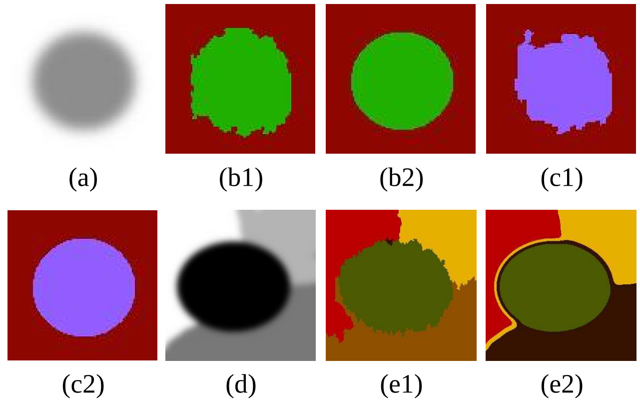

Figure 9. Comparison of the proposed region competition method with the region growing method in [15]. (a) Original image (100 * 100). (b1) Segmentation using the region growing method in [15], ν = 5000, CPU = 0.27s. (b2) Segmentation using the proposed model, ν = 5000, CPU = 0.33s. (c1) Segmentation using the region growing mothod in [15], ν = 12000, CPU = 0.26s. (c2) Segmentation using the proposed model, ν = 12000, CPU = 0.27s. (d) Original image (300 * 300). (e1) Segmentation of (d) using the region growing mothod in [15], $\nu = 18000$, CPU = 2.69s. (e2) Segmentation of (d) using the proposed model, $\nu = 18000$, CPU = 3.52s.

References

[1] V. Caselles, F. Catte, T. Coll, and F. Dibos. A geometric model for active contours. *Numerische Mathematik*, 66:1–31, 1993.

[2] V. Caselles, R. Kimmel, and G. Sapiro. Geodesic active contours. *Int. J. Comput. Vis.*, 22(1):61–79, 1997.

[3] T.F. Chan and L.A. Vese. Active contours without edges. *IEEE Trans. Image Processing*, 10(2):266–277, Feb. 2001.

[4] B. Chaudhuri and N. Sarkar. Texture segmentation using fractal dimension. *IEEE Trans. PAMI*, 17(1):72–77, Jan. 1995.

[5] M. Gage and R.S. Hamilton. The heat equation shrinking convex plane curves. *J. Differential Geometry*, 23:69–96, 1986.

[6] S. Gao and T.D. Bui. Image segmentation and selective smoothing by using mumford-shah model. *IEEE Trans. Image Processing*, 14(10):1537–1549, Oct. 2005.

[7] M. Grayson. The heat equation shrinks embedded plane curves to round points. *J. Differential Geometry*, 26:285–314, 1987.

[8] J.Chung and L. Vese. Image segmentation using a multilayer level-set approach. *UCLA CAM Report*, 3(53), Jun. 2005.

[9] J.Sethian. *Level Set Methods and Fast Marching Methods*. Cambridge Monograph on Applied and Computational Mathematics. Cambridge University Press, 1999.

[10] M. Kass, A. Witkin, and D. Terzopoulos. Snakes - active contour models. *International Journal of Computer Vision*, 1(4):321–331, 1987.

[11] S. Kichenassamy, A. Kumar, P. Olver, A. Tannenbaum, and A. Yezzi. Gradient flows and geometric active contour models. *Fifth Int. Conf. Computer Vision*, pages 810–815, 1995.

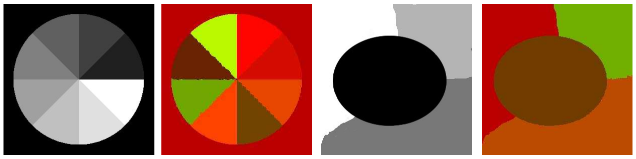

(a1) (a2) (b1) (b2)

Figure 10. More results of the proposed region competition method for complicated images. (a1) A biscuit image (300 * 300). (a2) Segmentation of (a1), ν=300, CPU =4.08s. (b1) An image with multiple junctions (300 * 300). (b2) Segmentation of (b1), ν = 2000, CPU = 5.02s.

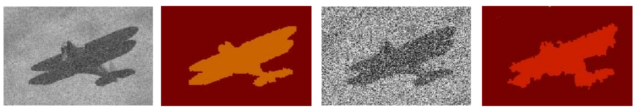

(a1) (a2) (b1) (b2)

Figure 11. Stability of the proposed region competition method w.r.t. noise. (a1)(b1) are original images (200 * 133), with noise becoming stronger. (a2) Segmentation of (a1), ν=1000, CPU =1.08s. (b2) Segmentation of (b1), ν = 3000, CPU = 8.85s.

(a1) (a2) (b1) (b2)

Figure 12. Extension of the proposed region competition method to color images. (a1)(b1) Color images (256 * 256). (a2) Segmentation of (a1), ν=1050, CPU =2.19s. (b2) Segmentation of (b1), ν = 1200, CPU = 2.05s.

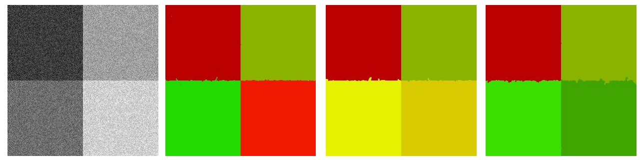

(a) (b) (c) (d)

Figure 13. Effects of ν on segmentation results. (a) A gray image with different distributions (300 * 300). (b)Segmentation of (a), $\nu = 800$, CPU = 24.79s. (c) Segmentation of (a), $\nu = 1200$, CPU = 10.29s. (d) Segmentation of (a), ν = 2000, CPU = 3.91s.

[12] B.B. Kimia, A.R. Tannenbaum, and S.W. Zucker. Shapes, shocks, and deformations I: the components of two-dimensional shape and the reaction-diffusion space. *Int. J. Comput. Vision*, 15(3):189–224, 1995.

[13] R. Kimmel. Fast edge integration. *Geometric Level Set Methods in Imaging, Vision, and Graphics, S. Osher and N. Paragios (Ed.), Springer*, pages 59–74, 2003.

[14] R. Malladi, J. Sethian, and B. Vemuri. Evolutionary fronts for topology independent shape modeling and recovery. *Proc. 3rd Eur. Conf. Computer Vision*, pages 3–13, 1994.

[15] Jean Michel Morel and Sergio Solimini. *Variational methods in image segmentation*. Birkhauser Boston Inc., Cambridge, MA, USA, 1995.

[16] D. Mumford and J. Shah. Optimal approximation by piecewise smooth functions and associated variational problems. *Comm. On Pure and Appl. Math.*, XLII:577–685, 1989.

[17] S. Osher and J. Sethian. Front propagating with curvature-dependent speed: algorithms based on hamilton-jacobi formulations. *J. Compu. Phys.*, 79:12–49, 1988.

[18] Y. Pan, J.D. Birdwell, and S.M. Djouadi. A new gradient and region based snake. *Proceedings of ICASSP2005, Philadelphia, PA, USA*, II:745–748, Mar. 2005.

[19] N. Paragios and R. Deriche. Coupled geodesic active regions for image segmentation: A level set approach. *Proceedings ECCV, Dublin*, V(II):224–240, 2000.

[20] Y. Shi and W.C. Karl. A fast level set method without solving pdes. *Proceedings of ICASSP 2005, Philadelphia, PA, USA*, II:97–100, Mar. 2005.

[21] H. Tek and B.B. Kimia. Shock-based reaction-diffusion bubbles for image segmentation. *Tech. Report LEMS-138*, Aug. 1994.

[22] A. Tijsseling. Gabor API. *http://www.kung-foo.tv/gaborapi.php*.

[23] A. Tsai, A. Yezzi, and A.S. Willsky. Curve evolution implementation of the mumford-shah func-

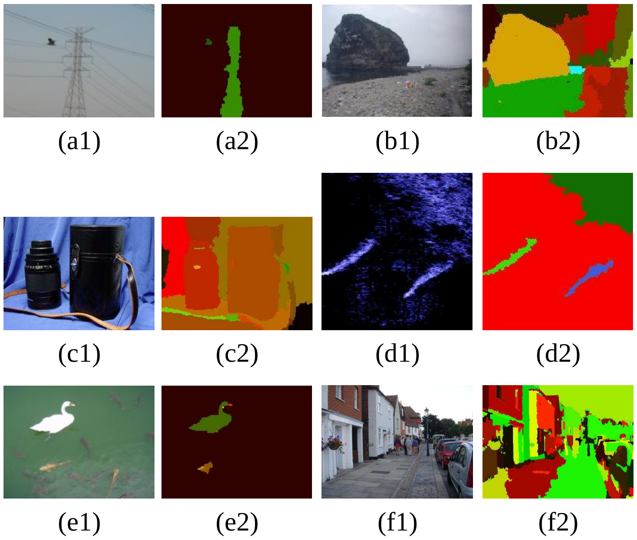

Figure 14. Experimental results of the proposed region competition method for real images. (a1)-(f1) are original real images. The sizes are: (a1) 200 * 150, (b1) 200 * 150, (c1) 300 * 225, (d1) 255 * 266, (e1) 200 * 150, (f1) 500 * 375. (a2)-(f2) are segmentation results of images (a1)-(f1). Corresponding parameters are: (a2) ν = 1500, CPU = 1.09s, (b2) ν = 2500, CPU = 1.06s, (c2) ν = 15000, CPU = 2.66s, (d2) ν = 7000, CPU = 4.61s, (e2) ν = 600, CPU = 1.82s, (f2) ν = 3000, CPU = 9.47s.

tional for image segmentation, denoising, interpolation, and magnification. *IEEE Trans. Image Processing*, 10(8):1169–1186, Aug. 2001.

[24] M.R. Turner. Texture discrimination by Gabor functions. *Biological Cybernetics*, 55:71–82, 1986.

[25] L.A. Vese and T.F. Chan. A mumtiphase level set framework for image segmentation using the mumford and shah model. *Inter. J. Computer Vision*, 50(3):271–293, 2002.

[26] A. Yezzi, A. Tsai, and A. Willsky. A fully global approach to image segmentation via coupled curve evolution equations. *Journal of Visual Communication and Image Representation*, 13:195 –216, 2002.

[27] S.C. Zhu and A. Yuille. Region competition: Unifying snakes, region growing, and bayes/mdl for multiband image segmentation. *IEEE Trans. PAMI*, 18(9):884–900, Sep. 1996.

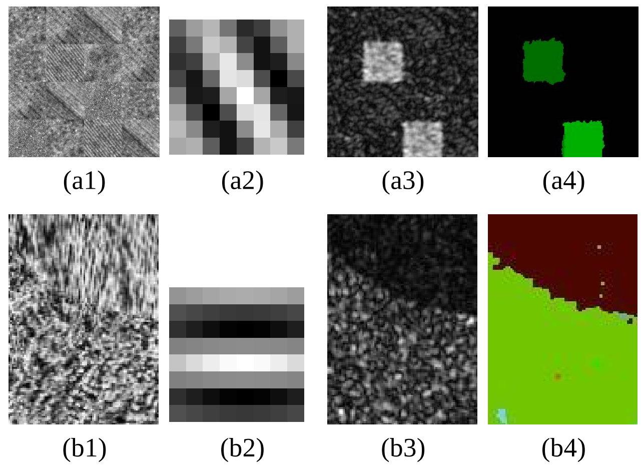

Figure 15. Texture segmentation using the proposed region competition model and Gabor filters. (a1)(b1) are original textured images. (a2)(b2) show the Gabor filters applied on original images. (a3)(b3) display the outputs of Gabor filters. (a4)(b4) represent the segmentation results for (a1)(b1) respectively.